

## SOLIDIFICATION BEHAVIOR AND ENVIRONMENTAL RISK ASSESSMENT OF TOXIC ELEMENTS ON TAILINGS FROM CARBOTHERMIC REDUCTION-MAGNETIC SEPARATION OF LEAD BLAST FURNACE SLAG

Z.-W. Jiang <sup>a,c</sup>, M.-T. Li <sup>a,b,\*</sup>, C. Wei <sup>a,b</sup>, Y.-L. Cao <sup>a</sup>, X.-B. Li <sup>a,b</sup>, Z.-G. Deng <sup>a,b</sup>

<sup>a</sup> Faculty of Metallurgy and Energy Engineering, Kunming University of Science and Technology, Kunming, China

<sup>b</sup> State Key Laboratory of Complex Nonferrous Metal Resources Clean Utilization, Kunming University of Science and Technology, Kunming, China

<sup>c</sup> Hunan Zhongke Electric Co.,Ltd, Yueyang, China

(Received 22 November 2022; Accepted 29 November 2023)

### Abstract

Lead blast furnace slag (LBFS) generated during lead smelting is a hazardous solid waste containing potentially toxic elements (Pb, Zn, As, and Cd) with high mobility and solubility. In this study, a process for the utilization of LBFS by carbothermic reduction-magnetic separation method is proposed. Leaching toxicity and Tessier sequential extraction experiments were conducted on LBFS and magnetic separation tailings (TS), and the environmental risk was evaluated using the risk assessment coding index and potential ecological risk index. The obtained results showed that the potentially toxic elements in the TS were solidified in the spinel phase or silicate phase. In addition, the XRD, SEM-EDS, and FTIR results showed the formation of  $PbCa_2Si_3O_9$ ,  $ZnAl_2O_4$ , and  $Ca_3(AsO_4)_2$  phases. The leaching concentrations of Pb, Zn, As, and Cd in TS were much lower than the toxicity characteristic leaching procedure (TCLP) and China standard leaching test (CSLT) limits. The results of Tessier sequential extraction procedure confirmed that the proportions of the stable residual state of the potentially toxic elements in TS were significantly higher than in LBFS. Furthermore, the ecological environmental risk level for the TS decreased significantly compared to that of LBFS.

**Keywords:** Lead blast furnace slag; Environmental risk; Potentially toxic elements; Carbothermic reduction; Magnetic separation; Leaching toxicity

### 1. Introduction

Metal smelting is considered to be the main source of heavy metal pollution, accompanied by the generation of waste gases, effluent, and solid waste [1]. In China, nearly 7100 t of waste slag is generated for every 10000 tons of lead and nearly 9600 t of waste slag is generated for every 10000 tons of zinc, and the traditional treatment method of slag is dumping [2]. Because of the scarcity of mineral resources, people started to pay attention to the extensive use of secondary resources such as smelting slag [3, 4]. On the other hand, smelting slag contains many heavy metals, the release of which leads to environmental pollution. Lead blast furnace slag (LBFS) is a hazardous solid waste generated in the lead smelter, and is difficult to flow and spread [5-7]. The main components of LBFS are FeO, SiO<sub>2</sub>, CaO, and Al<sub>2</sub>O<sub>3</sub>, while the balance mainly consists of Pb and Zn with small amounts of As and Cd. These potentially toxic elements with high mobility can

enter and accumulate in soil or water/sediment through rainwater leaching, weathering or human activities, posing a potential risk and damage to the ecological environment [8-10]. Heavy metals are very difficult to biodegrade. They are enriched under the biological amplification of the food chain, and they eventually enter the human body, leading to various diseases [11]. In China, a higher concentration of heavy metals has been detected in the hair of residents living near the lead smelting industries than in remote areas [12]. Therefore, the harmless and recycling treatment of LBFS can turn waste into treasure. In addition, it contributes to environmental protection and has good social and economic benefits [13].

Several technologies are currently used to treat LBFS, such as pyrometallurgical methods [14, 15], hydrometallurgical methods [16-18], and material preparation [19, 20]. Acid/alkali leaching is an effective method for the recovery of valuable metals. Wang [21] used sulfur or pyrite as the energy material of autotrophic organisms to leach metals from lead-

Corresponding author: liminting@163.com

<https://doi.org/10.2298/JMMB221022031J>



zinc smelting slag. The obtained results showed that the extraction efficiency of Zn, Cd, and In reached 90%, 86%, and 71%, respectively. However, the contents of Pb, As, and Ag in the leaching residue were too high, and the leaching residue can easily lead to secondary environmental pollution. These two methods are particularly effective for material preparation and solidification of LBFS when these toxic elements are combined into a form immune to leaching. Li et al. [22] prepared glass ceramics using lead fuming slag and waste glass, effectively stabilizing the heavy metals in the obtained glass ceramics with good physical, mechanical, and chemical properties. However, the use of curing agent increases the cost [23], and the valuable metals in the slag cannot be recovered. Pyrometallurgical treatment is another way of utilizing LBFS. It has been proven to be an effective method for recovering valuable metals from LBFS. Li et al. [24] studied the enhanced reduction effect of iron oxide on lead and zinc oxides in lead slag. At a temperature of 1550°C, a C/Fe molar ratio of 1.8, a holding time of 15 min, and a basicity of 1.2, the volatilization rates of lead and zinc reached 96.64% and 99.99%, respectively. This provides a clean technology for strengthening the reduction of lead and zinc oxides from smelting waste residue.

For the safe disposal of approximately 30000000 t of blast furnace slag that has accumulated in Gejiu City, Yunnan Province, a cost-effective treatment method which can effectively recover Pb, Zn, and Fe, perform the solidification of potentially toxic elements, and reduce the environmental risk of slag, should be developed. A carbothermic reduction-magnetic separation method was used for this purpose. The effects of temperature, holding time, magnetic field intensity and mass ratio of carbon to slag on the recovery of lead, zinc and iron were investigated. 91.9 wt% of Pb, 78.9 wt% of Fe and 97 wt% of Zn in LBFS were recovered by the reaction with carbon at 1300°C for 1h. Tailings (TS) and dust containing Pb and Zn, and iron powder with iron content of 90.95%, were

obtained according to the previous experimental results. This study focused on the leaching toxicity and speciation of potentially toxic elements in TS and LBFS, as well as the mineralogical characteristics of TS and LBFS. In order to understand how the mineralogical characteristics may affect the geochemical behavior of toxic elements, two typical evaluation models, the potential ecological risk index (RI) and risk evaluation coding index [25, 26], were used. Moreover, the immobilization mechanism of potentially toxic elements in the carbothermic reduction process was further detailed by characterization using X-ray diffraction (XRD), Fourier transform infrared spectroscopy (FTIR), and scanning electron microscopy energy dispersive spectrometer (SEM/EDS). This study provides basic data and scientific basis for the comprehensive utilization of tailings.

## 2. Experimental

### 2.1. Materials

In this paper LBFS were sampled from Yunnan Province, China. There are five large hazardous LBFS heaps there, and the particles of LBFS were pointed, hard, and dense. A representative sample was first collected from these five different slag heaps. The samples collected from each heap were then uniformly mixed in proportions. The TS came from carbothermic reduction-magnetic separation. The specific process is shown in Fig. 1. The LBFS was mixed with coke and sent to a high-temperature tubular furnace for the reduction reaction. The heating rate of the tubular furnace was set to 5 °C/min. Subsequently, the reduction slag was cooled down to 25°C and crushed, and the reduction slag was then separated into TS and iron powder by XCGS-50 magnetic separation tube. Under the best conditions of smelting temperature 1300 °C, a holding time of 60 min, a mass ratio of carbon to slag of 4% and a magnetic field intensity of 280KA/m, 91.9 wt% Pb, 78.9 wt% Fe and 97 wt% Zn

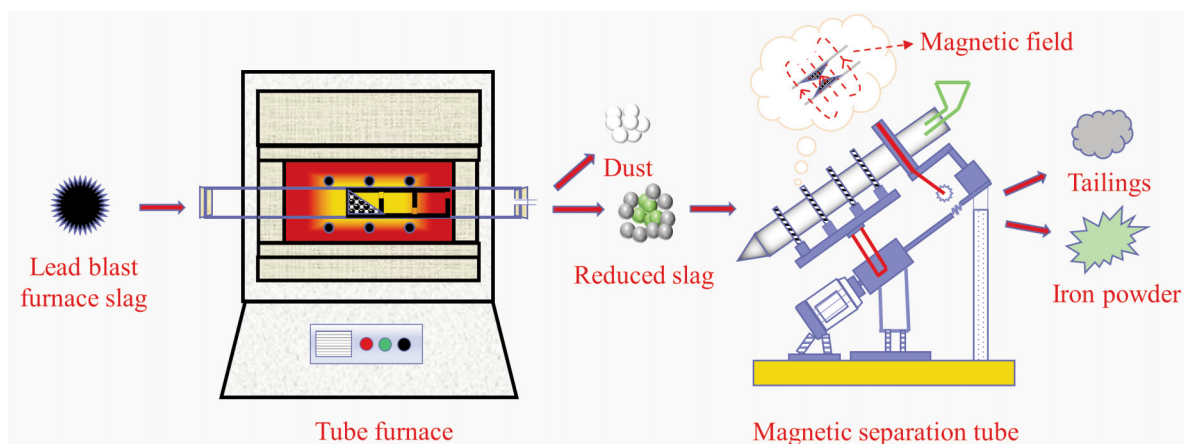


Figure 1. Source of Tailings

were recovered. The total metal concentration can indicate the total metal content. However, it cannot obtain complete information on their ecological risk and potential toxicity, and the existing form of metal determines its migration ability in the environment. Consequently, the environmental risk assessment and the solidification behavior of potentially toxic elements should be further studied. Note that distilled water and analytical grade chemical reagents were used for all experiments in this study.

## 2.2. Phase and mineralogy analysis

The XRD analysis was performed using Rigaku D/max-2200 diffractometer with Cu K $\alpha$  radiation ( $\lambda = 0.15406$  nm, 56 kV, 183 mA) at  $0.02^\circ$  intervals at  $10^\circ/\text{min}$  from  $5^\circ$  to  $90^\circ$ . The contents of the elements in all the digestion solutions obtained in this study were determined by inductively coupled plasma-atomic emission spectroscopy (ICP-OES), and an X-ray fluorescence (XRF) test conducted for the LBFS and TS. The microstructure and elemental composition of the LBFS and TS were analyzed by SEM (TESCAN MIRA LMS, Czech Republic) equipped with an EDS (Xplore). The chemical bonding structure of the samples was analyzed by FTIR spectra (Bruker Tensor 27, Germany). The phase composition analysis of lead and zinc in LBFS and TS were conducted by Kunming Metallurgical Research Institute using the chemical phase analysis method.

## 2.3. Environmental risk assessment method

### 2.3.1. Leaching test

The toxicity characteristic leaching procedure (TCLP) was investigated following the U.S. Environment Protection Agency [27], which is used to simulate the process of leaching waste components into groundwater under the condition of co-disposal of industrial solid waste and municipal solid waste. TCLP experiments were conducted using a buffered acetic acid as extraction solution, with a liquid-to-solid ratio of 20:1. The sulfuric acid and nitric acid method was performed according to the China standard leaching test (CSLT) [28] and was used to

**Table 1.** The Tessier extraction steps

Steps	Chemical forms	Extraction reagents	Reaction conditions
I	Exchangeable	1mol/L MgCl $_2$ , pH=7	Oscillate for 3h, 25°C
II	Bound to carbonates	1mol/L CH $_3$ COONa, pH=5	Oscillate for 5h, 25°C
III	Bound to Fe-Mn oxides	0.04mol/L NH $_2$ OH·HCl	Oscillate for 6h, 95°C
IV	Bound to organic matter	0.02mol/L HNO $_3$ +8.8mol/L H $_2$ O $_2$	Oscillate for 2h, 95°C
		8.8mol/L H $_2$ O $_2$ , pH=2	Oscillate for 3h, 95°C
		3.2mol/L CH $_3$ COONH $_4$	Oscillate for 0.5h, 25°C
V	Residual	HNO $_3$ +HF+HClO $_4$	Mixed acid digestion

simulate the migration characteristics of waste under acid precipitation. The extractant was a mixed solution of H $_2$ SO $_4$ :HNO $_3$  with a weight ratio of 2:1 and a liquid-to-solid ratio of 10:1. All the tests were oscillated at a rate of  $30\pm 2$  r/min for  $18\pm 2$  h in a polyethylene centrifuge tube at  $23\pm 2$  °C, and the leaching solution was then filtered using a 0.45-  $\mu\text{m}$  filter membrane. The concentrations of Pb, Zn, As, and Cd were analyzed by ICP-OES.

### 2.3.2. Sequential extraction procedure

The Tessier sequential extraction procedure of heavy metals [29] was proposed to analyze the binding forms of metals in soil or solid waste. The forms of heavy metals are divided into five types: exchangeable, bound to carbonates, bound to Fe-Mn oxides, bound to organic matter, and residual. The extraction difficulty of each binding state increased in turn, and the corresponding bioavailability decreased in turn. The steps of the sequential extraction procedure are presented in Table 1.

### 2.3.3. Risk assessment code (RAC)

The risk assessment code (RAC) was proposed to evaluate the bioavailability of metals in solid media [30].

$$RAC = \frac{C_m}{C_t} \cdot 100\% \quad (1)$$

where  $C_m$  represents the concentration of weak acid soluble metal and  $C_t$  represents the total concentration of a metal.

According to the proportion of weak acid soluble state in the total amount, the classification of risk is divided into five levels. In addition, the higher the RAC value, the higher the environmental risk level. Five categories of RAC were defined (Table 2).

### 2.3.4. Potential ecological risk index (RI)

RI was proposed to describe the characteristics of bioavailability and relative contribution ratio, and reflect the potential influence of heavy metals in



**Table 2.** The RAC risk level

Value of RAC	Environmental risk level
RAC<1%	No risk
1%<RAC<10%	Low risk
11%<RAC<30%	Moderate risk
31%<RAC<50%	High risk
50%<RAC	Extremely high risk

sediments [31]. Different metals will cause different ecological hazards. The RI formulas are given by:

$$RI = \sum E_r^i = \sum T_r^i C_n^i \quad (2)$$

$$C_n^i = \frac{C_s^i}{C_r^i} \quad (3)$$

where  $E_r^i$  represents the potential ecological hazard index of a given metal,  $T_r^i$  is the toxicity response factor for a given metal, while the coefficients based on its toxicity are Pb = 5, Zn = 1, As = 10, and Cd = 30 [32, 33],  $C_n^i$  is the pollution index for a certain metal,  $C_s^i$  represents the measured concentration of metal elements to be evaluated, and  $C_r^i$  is the reference value of metal background while the background values for Pb, Zn, As, and Cd are 500, 500, 40, and 1.0, respectively [34].

The pollution degree and potential ecological risk classification corresponding to each parameter were shown in Table 3.

### 3. Results and discussion

#### 3.1. Characterization analysis of LBFS and TS

##### 3.1.1. Chemical compositions

The chemical compositions of the LBFS and TS are presented in Table 4. The results show that the main components of LBFS are Fe, SiO<sub>2</sub>, and CaO, and that the potentially toxic elements mainly include Pb, Zn, As, and Cd. The main gangue components of TS are SiO<sub>2</sub>, CaO, and Al<sub>2</sub>O<sub>3</sub>, that have the potential of material utilization. The total content of Pb, Zn, As, and Cd in TS is significantly lower than that in LBFS, which indicates that Pb and Zn are effectively volatilized and recovered, and Fe is recovered by magnetic separation. Table 5 shows the phase composition analysis of Pb and Zn in LBFS and TS.

**Table 4.** Chemical compositions of LBFS and TS (wt./%)

Materials	Pb	Zn	As	Cd	Fe	SiO <sub>2</sub>	CaO	Al <sub>2</sub> O <sub>3</sub>
LBFS	3.74	3.84	0.88	0.032	30.83	25.14	10.55	6.85
TS	0.72	0.28	0.20	0.005	10.50	38.05	12.05	8.20

**Table 5.** Phase composition of lead and zinc in LBFS and TS (wt. /%)

Sample	Phase of Lead				Phase of Zinc			
	PbSO <sub>4</sub>	PbCO <sub>3</sub>	PbS	Plumbojarosite	ZnSO <sub>4</sub>	ZnO	ZnS	Franklinite
LBFS	0.96	0.86	0.98	0.94	0.30	1.47	1.73	0.34
TS	0.302	0.107	0.266	0.045	0.01	0.13	0.07	0.01

The proportions of all the lead phases in LBFS are approximately equal, and Zn is mainly sulfide and oxide. The sulfide and sulfate of Pb account for more than 78% of the lead phase, and more than 46% of Zn in the zinc phase exists in the form of oxide in TS.

##### 3.1.2. Mineralogical compositions

The XRD patterns of the LBFS and TS fractions are used to analyze the evolution of the main crystal types during the transformation of LBFS to TS (Fig. 2). The main mineral composition of LBFS includes magnetite (Fe<sub>3</sub>O<sub>4</sub>), sphalerite (ZnS), monticellite (CaMgSiO<sub>4</sub>), and alumina (Al<sub>2</sub>O<sub>3</sub>), and amorphous phases were observed at 5°-20° (2θ max CuKα). Some new phases of gahnite (ZnAl<sub>2</sub>O<sub>4</sub>), margarosanite (PbCa<sub>2</sub>Si<sub>3</sub>O<sub>9</sub>) and calcium arsenite (Ca<sub>3</sub>(AsO<sub>4</sub>)<sub>2</sub>) were observed in the TS. The crystal structure type affects the solidification efficiency of heavy metals, and the stable crystal structure confers greater strength and chemical stability [36]. The appearance of PbCa<sub>2</sub>Si<sub>3</sub>O<sub>9</sub>, ZnAl<sub>2</sub>O<sub>4</sub>, and Ca<sub>3</sub>(AsO<sub>4</sub>)<sub>2</sub> indicates that the TS has very good solidification of Pb, Zn, and As. In addition, the chemical phase of Cd cannot be found.

##### 3.1.3. Chemical construction

Fig. 3 presents the FTIR spectral curves of LBFS and TS. The bending vibration near 1622 cm<sup>-1</sup> is the characteristic of the O-H bond [37, 38], which is due to the fact that the LBFS stacked in an open area contains H<sub>2</sub>O molecules. The bands at 880 cm<sup>-1</sup> are

**Table 3.** The relationship between potential ecological hazard index and risk level

$E_r^i$		RI	
$E_r^i < 40$	Low risk	RI < 150	Low risk
$40 \leq E_r^i < 80$	Moderate risk	$150 \leq RI < 300$	Moderate risk
$80 \leq E_r^i < 160$	Higher risk	$300 \leq RI < 600$	High risk
$160 \leq E_r^i < 320$	High risk	RI ≥ 600	Serious risk
$E_r^i \geq 320$	Serious risk	/	/



attributed to the bending vibration of Si-O. The stretching vibration of Si-O-Al(Si) is  $971\text{ cm}^{-1}$  (TS) and it is shifted compared to  $880\text{ cm}^{-1}$  (LBFS). This may be related to the heavy metal ions replacing the charge balancing ions (i.e.,  $\text{Na}^+$  and  $\text{Ca}^+$ ) [39, 40]. The bands at  $478\text{ cm}^{-1}$  and  $501\text{ cm}^{-1}$  are due to the bending vibrations of Si-O-Si and O-Si-O in tetrahedral silicate [41, 42], and the shift of the absorption peak at  $478\text{ cm}^{-1}$  to  $501\text{ cm}^{-1}$  may be caused by the change of crystalline phases. In addition, the peak near  $736\text{ cm}^{-1}$  may be due to the bending vibration of Al-O in  $[\text{AlO}_4]$  of the crystalline phase [43].

### 3.1.4. Solidifying characteristics and element distribution

The mechanism of elemental reduction and solidification in the carbothermic reduction process is shown in Fig. 4. Pb, Zn, As, and Cd are reduced then fed into the gas phase and recovered in the form of dust. In addition, Fe enters the metal phase and stratifies with the slag phase. Moreover, the potentially toxic elements remained in the slag phase enter the silicate structure for stabilization.

The element distribution and microstructure of LBFS are shown in Fig. 5. The SEM image shows that LBFS is amorphous and irregular, and that small grain aggregates exist on the surface of bulky grain. From the distribution of surface scanning elements in Fig. 5(A) and the EDS results in Table 6, it can be inferred that the distribution of Pb, Zn, As, and Cd mostly coincides with that of Fe, and there is no clear aggregation trend, indicating that the potentially toxic elements in the slag are relatively dispersed mostly with the aggregation of iron compounds. This is due to the fact that heavy metals mainly exist in the form of Fe-Mn oxide particles, which is consistent with the speciation analysis results of heavy metals. The morphology and element distribution of TS are

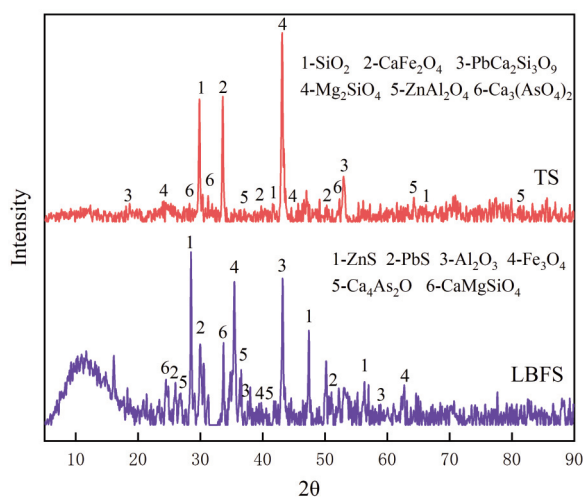


Figure 2. X-ray diffraction patterns for LBFS and TS

presented in Fig. 6. The glass phase structure is embedded with metal (point 1 in Fig. 6(A)), which is mainly composed of Pb and Fe (Table 6), and other elements such as Zn, As, and Cd are not found. It can be assumed that most of the  $\text{Pb}^{2+}$  ions enter the silicate phase. A solid solution structure composed of Si, Ca, Al and O can be seen in Fig. 7(B), in which Pb, Zn, As, and Cd can be found. The connection between Ca, Al, Si, O, Pb or Zn, reflects the compacted structure of Si-O-Ca-O and the existence of  $\text{PbCa}_2\text{Si}_3\text{O}_9$ ,  $\text{ZnAl}_2\text{O}_4$  and  $\text{Ca}_3(\text{AsO}_4)_2$ . From this it can be deduced that heavy metal ions enter the stable glass phase by replacing other elements in the process of carbothermic reduction. According to the Hume-Rothery rule, the smaller the difference between the ionic radius or electronegativity, the easier it is to form a displacement solid solution. The ionic radius and electronegativity of Pb, Zn, As, and Cd as well as the common ions  $\text{Ca}^{2+}$ ,  $\text{Si}^{4+}$ ,  $\text{Al}^{3+}$ ,  $\text{Mg}^{2+}$ , and  $\text{Fe}^{3+}$  are presented in Table 7. The  $\text{Pb}^{2+}$  and  $\text{Cd}^{2+}$  ions can easily form a substitutional solid solution with  $\text{Ca}^{2+}$ .  $\text{Zn}^{2+}$  and  $\text{Mg}^{2+}$ , as well as  $\text{As}^{3+}$  and  $\text{Fe}^{3+}$ , also have similar properties. In existing studies [44],  $\text{Si}^{4+}$  and  $\text{Al}^{3+}$  are

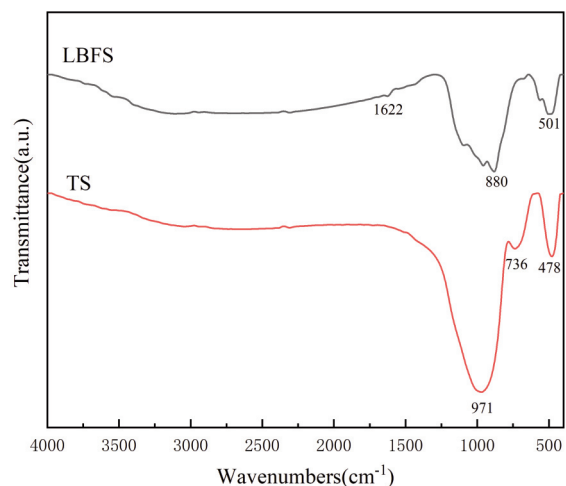


Figure 3. The FTIR spectra of LBFS and TS

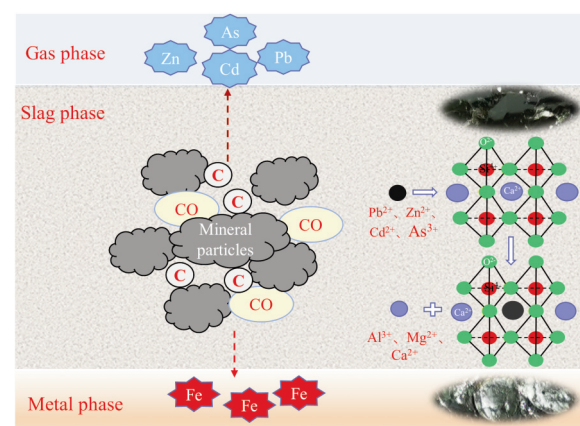


Figure 4. Element reduction and solidification mechanism



[SiO<sub>4</sub>] or [AlO<sub>4</sub>] can be replaced by heavy metals to form stable chemical bonds.

### 3.2. Leaching characteristics

The leaching concentration and the threshold value of potentially toxic elements in LBFS and TS are presented in Table 8. For LBFS, the leaching concentration of Cd in TCLP and CSLT exceeded the standard value of 1.00, and the leaching concentrations of Pb and As obtained from TCLP were well above the threshold values, with a concentration of 120 mg/L and 11.81 mg/L, respectively. The high content of alkali metal Fe in the slag had a strong buffer effect on reducing the leaching of heavy metals under acidic conditions. Therefore, the leaching values of Pb, Zn, As, and Cd in TCLP were greater than those in CSLT. The results show that LBFS is a hazardous waste which that causes serious pollution if it is directly piled in the natural environment. For TS, the leaching concentrations of Pb, Zn, As, and Cd in TCLP and

CSLT were significantly below the threshold values. This is due to the fact that most of the Pb, Zn, and Cd volatilized into the dust, resulting in a lower content of potentially toxic elements in TS. Moreover, most of the elements existed in a stable form, making it difficult to leach Pb, Zn, As, and Cd. In this situation, the slag sample had low environmental risk and appeared to be safe.

### 3.3. Speciation of Pb, Zn, As, and Cd

The speciation and distribution of potentially toxic elements affect leaching toxicity and biosafety. The exchangeable state is very sensitive to environmental changes and can easily migrate and transform. The carbonate bound state is most sensitive to the pH value change and can be released through weak acid. The Fe-Mn oxide bound state is wrapped by Fe-Mn oxide or hydroxide, which is generally present as fine dispersed particles. However, it can easily lead to secondary pollution

Table 6. EDS results of samples in Fig 5-6

Weight/% Number	Si	Ca	Fe	O	Pb	Zn	As	Cd	Al	S
A	4.6	2.9	37.6	26.9	8.5	5.0	1.8	0.2	1.12	5.6
B	18.34	12.39	10.86	42.36	1.07	1.06	0.38	0.43	6.17	2.31

Table 7. The ionic radius and electronegativity of the metal

Ion species	Si <sup>4+</sup>	Ca <sup>2+</sup>	Al <sup>3+</sup>	Fe <sup>3+</sup>	Mg <sup>2+</sup>	Pb <sup>2+</sup>	Zn <sup>2+</sup>	As <sup>3+</sup>	Cd <sup>2+</sup>
Ion radius(nm)	0.04	0.1	0.054	0.0645	0.072	0.119	0.074	0.058	0.095
Electronegativity	1.74	1.04	1.47	1.64	1.20	1.26	1.65	2.18	1.46

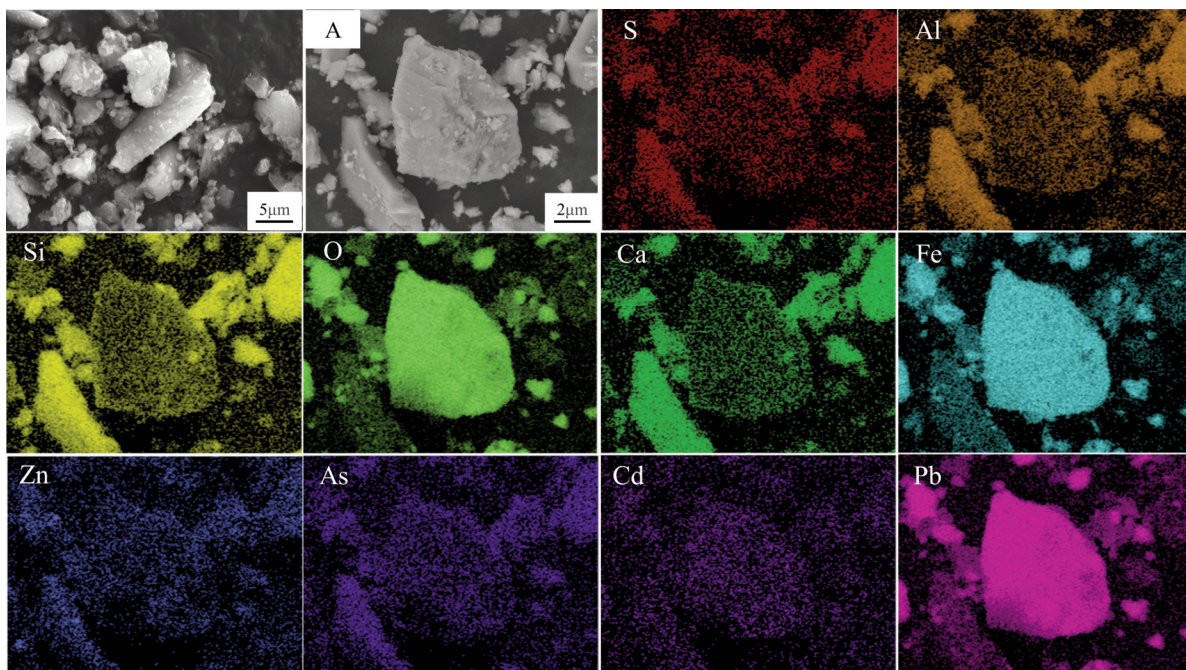


Figure 5. SEM/EDS image of LBFS

when the pH value and redox potential are reduced. The organic bound state refers to the metal chelated or complexed by organic matter, which is relatively stable under natural conditions. The residue state generally exists in a silicate lattice, which is very stable under natural conditions, and it has the lowest toxicity and biological activity of the five forms. Fig. 7 presents the speciation of Pb, Zn, As, and Cd in LBFS and TS as a percentage of the total concentration, showing the composition characteristics of potentially toxic elements.

The main forms of Pb, Zn, As, and Cd in LBFS were iron manganese oxides, which was related to the high iron content. The percentages of heavy metals in the exchangeable state ranging from the highest to the lowest were: Cd > Zn > Pb > As. The proportions of Pb, Zn, and As in the exchangeable state were less than 1%, and that of Cd in the exchangeable state reached 6.58%. The percentages of heavy metals in the carbonate bound state ranging from the highest to the lowest were: Pb > Cd > Zn > As. The binding ability of Pb to carbonate was greater than that of the other metals, accounting for 39.76%. The percentages of heavy metals in the Fe-Mn oxides

state ranging from the highest to the lowest were: Zn > As > Pb > Cd, and they were 72.73%, 60.46%, 45.71%, and 44.85%, respectively. Zn had a strong binding force with Fe-Mn oxide, due to the fact that Fe-Mn oxides have a strong wrapping effect on heavy metals. The percentages of heavy metal in the organic state ranging from the highest to the lowest were: As > Zn > Cd > Pb. The percentages of heavy metal in the residue state ranging from the highest to the lowest were: Cd > As > Zn > Pb. The contents of Cd and As in the residue were respectively 26.2% and 16.2%, while those of Pb and Zn were only 2.4% and 4.54%, respectively. This indicates that the environmental risks of Pb and Zn were highest in LBFS. In addition, the environmentally effective states of Pb, Zn, As and Cd in LBFS accounted for more than 70%.

The order of the content of potentially toxic elements in the exchangeable state was: Cd > Pb > As > Zn in TS, and the percentage content was between 1% and 5%. The content of potentially toxic elements in the carbonate bound state was Pb > Cd > Zn > As, and the proportion of Pb in the carbonate bound state was 12.15%. The order of potentially

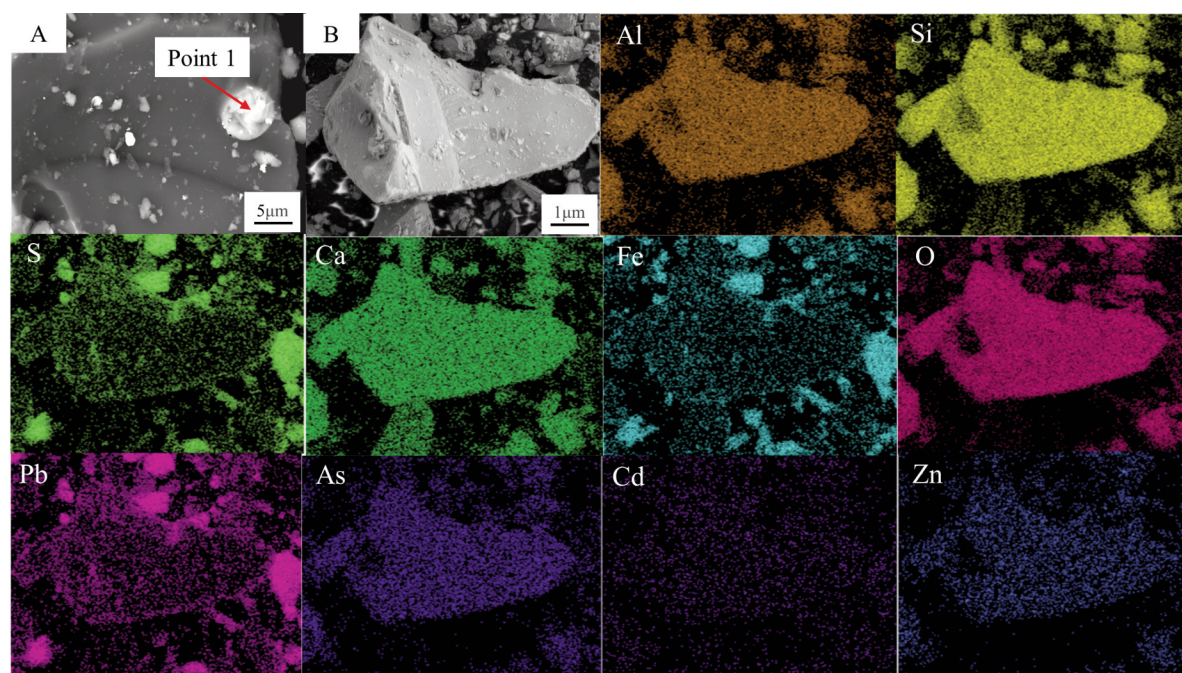


Figure 6. SEM/EDS image of TS

Table 8. Metal concentrations based on TCLP and CSLT leaching test

Sample	TCLP/(mg·L <sup>-1</sup> )				CSLT/(mg·L <sup>-1</sup> )			
	Pb	Zn	As	Cd	Pb	Zn	As	Cd
LBFS	120	50.28	11.81	3.22	1.07	16.46	0.39	1.91
TS	0.27	0.84	0.02	0.05	0.10	0.10	0.044	0.018
Threshold value	5.00	/	5.00	1.00	5.00	100.00	5.00	1.00



toxic elements content of the Fe-Mn oxides state was Pb > As > Zn > Cd, and the percentages were 43.38%, 43.09%, 40.41% and 35.56%, respectively. The order of potentially toxic elements content in the organic state was Zn > Cd > As > Pb. The order of potentially toxic elements content in the residue state was As > Cd > Zn > Pb, and the percentages were 29.5%, 29.31%, 25% and 24.81%, respectively. Compared with LBFS, the environmentally effective state of potentially toxic elements in TS was reduced to different degrees, especially that of Pb and Zn.

There were some differences in the morphological distribution of potentially toxic elements between LBFS and TS. The proportions of the residual states of Pb, Zn, As, and Cd in TS were higher than those in LBFS, indicating that the risk of heavy metals release from TS to the environment was lower, and it has a good effect on the control of the Pb, Zn, As, and Cd pollution.

**3.4. Ecological risk assessment based on RI and RAC**

Fig. 8 shows the potential ecological risks of toxic elements in the LBFS and TS. From the perspective

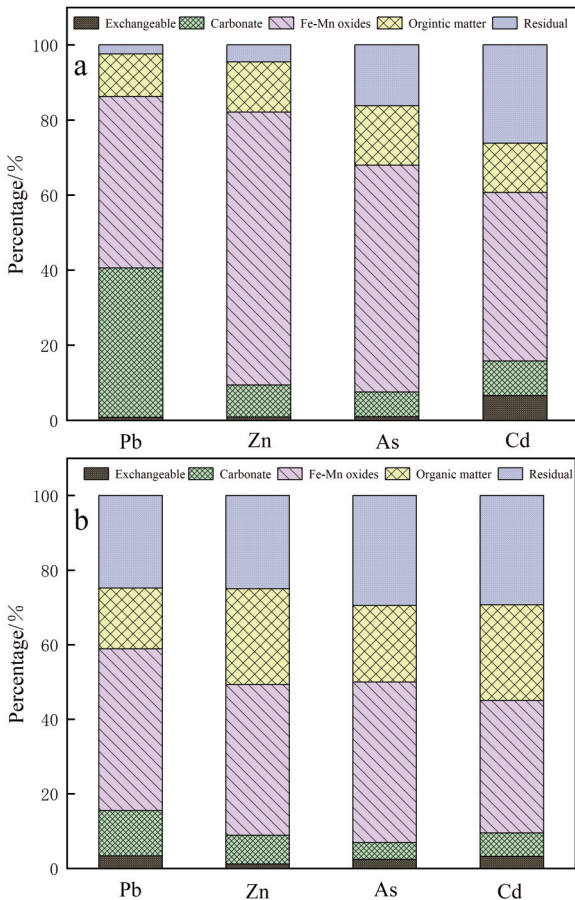


Figure 7. Speciation of potentially toxic elements in LBFS (a) and TS (b)

of bioavailability and migration and release risk of occurrence forms of heavy metals, the RAC values of potentially toxic elements for LBFS and TS had the following order: Pb > Cd > Zn > As. The risk level of Pb in LBFS was high, Cd presented a medium risk, and the environmental risks of Zn and As were low. Compared with LBFS, the risk level of Pb in TS was reduced from high to medium, that of Cd was reduced from medium to low, and that of Zn and As was low.

The potential ecological risk assessment results of toxic elements in LBFS and TS are shown in Table 9, which reflects the toxicity difference of different elements and the sensitivity of the environment to heavy metals pollution. The RI value of LBFS was  $1.23 \times 10^4$ , which corresponds to an extremely high risk. The contribution rates of the potentially toxic elements for RI had the following order: Cd > As > Pb > Zn. For the latter, the single element potential ecological hazard coefficient ( $E_r^i$ ) values of Cd and As were 9600 and 2200, respectively, which represents a serious threat to the environment, while only Zn presents a medium risk. The RI value of TS was  $1.83 \times 10^3$ , an order of magnitude lower than that of LBFS. However, it still presented a very high risk. This is mainly because the  $E_r^i$  value of Cd reached 1500. Furthermore, As, Pb, and Zn showed high, medium and low risks, respectively.

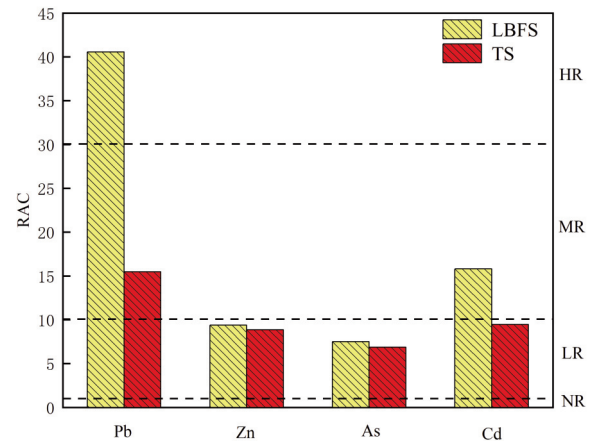


Figure 8. The calculated RAC values of the potentially toxic elements in the LBFS and TS

Table 9. Potential ecological risk indices of single elements and RI for samples

Sample	$E_r^i$				RI
	Pb	Zn	As	Cd	
LBFS	374	76.8	2200	9600	$1.23 \times 10^4$
TS	79	5.6	250	1500	$1.83 \times 10^3$



#### 4. Conclusion

In this study, LBFS was treated by high temperature carbothermal reduction-magnetic separation to obtain dust containing Pb and Zn, iron powder, and stabilized TS. Subsequently, the environmental risks of LBFS and TS, and the solidification behavior of potentially toxic elements were investigated.

(1) The method of carbothermic reduction-magnetic separation can effectively recover Pb, Zn, and Fe. The plumbojarosite phase is largely reduced and decomposed, and the ZnO is less reduced in LBFS. The potentially toxic elements in TS solidify in spinel or silicate state, which is caused by the heavy metal ions entering the glass phase to form substitutional solid solution or interstitial solid solution. Pb, Zn, and As are mainly present in  $\text{PbCa}_2\text{Si}_3\text{O}_9$ ,  $\text{ZnAl}_2\text{O}_4$ , and  $\text{Ca}_3(\text{AsO}_4)_2$  phases respectively, and show good stability.

(2) In the leaching experiments of TCLP and CSLT, the leaching concentrations of Pb, Zn, As, and Cd in TS are significantly lower than those of LBFS, and the concentration of potentially toxic elements in TS is in line with the safety standard value indicating that TS can be used for construction.

(3) Pb, Zn, As, and Cd are transformed into more stable components after carbothermic reduction. Compared with LBFS, the residual state of Pb, Zn, As and Cd in TS accounts for a larger percentage, and the environmental risk of TS is lower.

(4) The ecological risk level of Pb in LBFS is high, and the potential ecological risk level of each element in TS is below the medium. The RI value of LBFS is  $1.23 \times 10^4$ , in which the contributions of Cd and As are the largest. The RI value of TS is  $1.83 \times 10^3$ , with Cd being the main donor. In general, the potential environmental risk of TS is lower than that of LBFS.

In summary, the carbothermic reduction-magnetic separation can perform the volatilization and recovery of Pb and Zn in LBFS and the resource utilization of Fe. In addition, the potentially toxic elements are solidified in tailings and create the conditions for their material utilization, which reduces the environmental risk of the smelting slag.

#### Acknowledgements

*This work was supported by the natural science foundation of Yunnan Province, China (No.: 202101AT070091).*

#### Author Contributions

*Conceptualization, Methodology, Software, Investigation, Writing-Original Draft, Ziwei Jiang; Conceptualization, Methodology, Software,*

*Investigation, Minting Li; Resources, Supervision, Yinlei Cao, Xingbin Li, Zhigan Deng; The first draft of the manuscript was written by Ziwei Jiang and all authors commented on previous versions of the manuscript. All authors have read and approved the final manuscript.*

#### Data availability Statement

*The data that we used in this study can be requested by contacting the corresponding author.*

#### Declarations of interest

*The authors declare that they have no conflict of interest.*

#### References

- [1] D.G.Liu, X.B.Min, Y.Ke, L.Y.Chai, Y.J.Liang, Y.C.Li, Z.B.Wang, Co-treatment of flotation waste, neutralization sludge, and arsenic-containing gypsum sludge from copper smelting: solidification/stabilization of arsenic and heavy metals with minimal cement clinker, *Environmental Science and Pollution Research*, 25(8) (2018) 7600-7607. <https://doi.org/10.1007/s11356-017-1084-x>
- [2] D.M.Xu, R.B.Fu, Y.H.Tong, D.L.Shen, X.P.Guo, The potential environmental risk implications of heavy metals based on their geochemical and mineralogical characteristics in the size-segregated zinc smelting slags, *Journal of Cleaner Production*, 315 (1) (2021) 128199. <https://doi.org/10.1016/j.jclepro.2021.128199>
- [3] H.Shen, E.Forssberg, An overview of recovery of metals from slags, *Waste Management*, 23 (10) (2003) 933-949. [https://doi.org/10.1016/S0956053X\(02\)00164-2](https://doi.org/10.1016/S0956053X(02)00164-2)
- [4] P.Zhang, F.Muhammad, L.Yu, M.Xia, D.Li, Self-cementation solidification of heavy metals in lead-zinc smelting slag through alkali-activated materials, *Construction and Building Materials*, 249 (2020) 118756. <https://doi.org/10.1016/j.conbuildmat.2020.118756>
- [5] Y.Guan, G.Huang, L.Liu, M.Zhai, B.Zheng, Dynamic analysis of industrial solid waste metabolism at aggregated and disaggregated levels, *Journal of Cleaner Production*, 221 (1) (2019) 817-827. <https://doi.org/10.1016/j.jclepro.2019.01.271>
- [6] L.Zhang, H.Zhou, X.Chen, G.Liu, C.Jiang, L.Zheng, Study of the micromorphology and health risks of arsenic in copper smelting slag tailings for safe resource utilization, *Ecotoxicology and Environmental Safety*, 219 (2021) 112321. <https://doi.org/10.1016/j.ecoenv.2021.112321>
- [7] D.A.Pan, L.Li, X.Tian, Y.Wu, N.Cheng, H.Yu, A review on lead slag generation, characteristics, and utilization, *Resources, Conservation & Recycling*, 146 (2019). <https://doi.org/10.1016/j.resconrec.2019.03.036>
- [8] Y.Yang, S.Li, X.Bi, P.Wu, T.Liu, F.Li, C.Liu, Lead, Zn, and Cd in slags, stream sediments, and soils in an abandoned Zn smelting region, southwest of China, and Pb and S isotopes as source tracers, *Journal of Soils*



- and Sediments, 10 (8) (2010) 1527-1539. <https://doi.org/10.1007/s11368-010-0253-z>
- [9] L.Tang, C.Tang, J.Xiao, P.Zeng, M.Tang, A cleaner process for valuable metals recovery from hydrometallurgical zinc residue, *Journal of Cleaner Production*, 201 (2018) 764-773. <https://doi.org/10.1016/j.jclepro.2018.08.096>.
- [10] H.Akasaka, T.Takahata, I.Toda, H.Ono, S.Ohshio, S.Himeno, H.Saitoh, Hydrogen storage ability of porous carbon material fabricated from coffee bean wastes, *International Journal of Hydrogen Energy*, 36 (1) (2011) 580-585. <https://doi.org/10.1016/j.ijhydene.2010.09.102>
- [11] S.Çoruh, O.N.Ergun, Use of fly ash, phosphogypsum and red mud as a liner material for the disposal of hazardous zinc leach residue waste, *Journal of hazardous materials*, 173 (1-3) (2010) 468-473. <https://doi.org/10.1016/j.jhazmat.2009.08.108>
- [12] H.Li, C.Tan, L.Wu, Z.Zhang, Y.Jin, Z.Yang, Mechanochemical immobilization of lead smelting slag using quartz sand, *Minerals Engineering*, 151 (7) (2020) 106303. <https://doi.org/10.1016/j.mineng.2020.106303>
- [13] K.Q.Jiang, Z.H.Guo, X.Y.Xiao, L.Zhang, Extraction of metals from a zinc smelting slag using two-step procedure combining acid and ethylene diaminetetraacetic acid disodium, *Journal of Central South University*, 19 (7) (2012) 1808-1812. <https://doi.org/10.1007/s11771-012-1212-1>
- [14] Y.X.Zheng, W.Liu, W.Q.Qin, Y.Kong, H.L.Luo, J.W.Han, Mineralogical reconstruction of lead smelter slag for zinc recovery, *Separation science and technology*, 49 (5) (2014) 783-791. <https://doi.org/10.1080/01496395.2013.863342>
- [15] Q.Liu, C.Q.Wang, J.Tan, Z.L.Yin, Q.Y.Chen, Z.Liao, Y.Liu, Recovery of iron from lead-zinc metallurgical slags by bath smelting, *Journal of Central South University*, 22 (4) (2015) 1256-1263. <https://doi.org/10.1007/s11771-015-2641-4>
- [16] H.Yuan, Q.Liu, Z.Zhang, Germanium and Indium Leaching by Sulfuric Acid from a Zinc Smelting Slag in Yunnan, *Metal Mine*, 45 (07) (2016) 189. <https://doi.org/10.3969/j.issn.1001-1250.2016.07.037>
- [17] A.Ma, X.Zheng, S.Li, Y.Wang, S.Zhu, Zinc recovery from metallurgical slag and dust by coordination leaching in  $\text{NH}_3\text{-CH}_3\text{COONH}_4\text{-H}_2\text{O}$  system, *Royal Society open science*, 5 (7) (2018) 180660. <https://doi.org/10.1098/rsos.180660>
- [18] K.Gargul, B.Boryczko, A.Bukowska, Hydrometallurgical recovery of lead from direct-to-blister copper flash smelting slag, *Archives of Civil and Mechanical Engineering*, 17 (4) (2017) 905-911. <https://doi.org/10.1016/j.acme.2017.04.004>
- [19] S.K.Behera, C.N.Ghosh, K.Mishra, D.P.Mishra, P.Singh, P.K.Mandal, M.K.Sethi, Utilisation of lead-zinc mill tailings and slag as paste backfill materials, *Environmental Earth Sciences*, 79 (16) (2020) 1-18. <https://doi.org/10.1007/s12665-020-09132-x>
- [20] C.Atzeni, L.Massidda, U.Sanna, Use of granulated slag from lead and zinc processing in concrete technology, *Cement & Concrete Research*, 26 (9) (1996) 1381-1388. [https://doi.org/10.1016/0008-8846\(96\)00121-4](https://doi.org/10.1016/0008-8846(96)00121-4)
- [21] J.Wang, Q.Huang, T.Li, B.Xin, S.Chen, X.Guo, Y.Li, Bioleaching mechanism of Zn, Pb, In, Ag, Cd and As from Pb/Zn smelting slag by autotrophic bacteria, *Journal of Environmental Management*, 159 (15) (2015) 11-17. <https://doi.org/10.1016/j.jenvman.2015.05.013>
- [22] L.Li, Y.Wu, T.Liu, H.Yu, Characteristics and properties of glass-ceramics using lead fuming slag, *Journal of Cleaner Production*, 175 (20) (2018) 251-256. <https://doi.org/10.1016/j.jclepro.2017.12.030>
- [23] Y.Zhang, S.Zhang, W.Ni, Q.Yan, W.Gao, Y.Li, Immobilisation of high-arsenic-containing tailings by using metallurgical slag-cementing materials, *Chemosphere*, 223 (2019) 117-123. <https://doi.org/10.1016/j.chemosphere.2019.02.030>
- [24] Y.Li, Z.Liu, H.Liu, B.Peng, Clean strengthening reduction of lead and zinc from smelting waste slag by iron oxide, *Journal of Cleaner Production*, 143 (2017) 311-318. <https://doi.org/10.1016/j.jclepro.2016.12.108>
- [25] H.N.Zhu, X.Z.Yuan, G.M.Zeng, M.Jiang, J.Liang, C.Zhang, H.W.Jiang, Ecological risk assessment of heavy metals in sediments of Xiawan Port based on modified potential ecological risk index, *Transactions of Nonferrous Metals Society of China*, 22 (6) (2012) 1470-1477. [https://doi.org/10.1016/S1003-6326\(11\)61343-5](https://doi.org/10.1016/S1003-6326(11)61343-5)
- [26] M.S.Islam, M.K.Ahmed, M.Habibullah-Al-Mamun, Geochemical speciation and risk assessment of heavy metals in sediments of a river in bangladesh, *Soil and Sediment Contamination: An International Journal*, 24 (6) (2015) 639-655. <https://doi.org/10.1080/15320383.2015.997869>
- [27] S.E.Musson, Y.C.Jang, T.G.Townsend, I.H.Chung, Characterization of lead leachability from cathode ray tubes using the toxicity characteristic leaching procedure, *Environmental Science & Technology*, 34 (20) (2000) 4376-4381. <https://doi.org/10.1021/es0009020>
- [28] Y.L.Chen, X.Y.Guo, Q.M.Wang, Q.H.Tian, J.X.Zhang, S.B.Huang, Physicochemical and environmental characteristics of alkali leaching residue of wolframite and process for valuable metals recovery, *Transactions of Nonferrous Metals Society of China*, 32 (5) (2022) 1638-1649. [https://doi.org/10.1016/S1003-6326\(22\)65899-0](https://doi.org/10.1016/S1003-6326(22)65899-0)
- [29] A.P.G.C.Tessier, P.G.Campbell, M.J.A.C.Bisson, Sequential extraction procedure for the speciation of particulate trace metals, *Analytical Chemistry*, 51 (7) (1979) 844-851. <https://doi.org/10.1021/ac50043a017>
- [30] G.Perin, L.Craboleda, M.Lucchese, R.Cirillo, L.Dotta, M.L.Zanette, A.A.Orio, Heavy metal speciation in the sediments of Northern Adriatic Sea, A new approach for environmental toxicity determination, *Heavy Metals in the Environment*, 2 (1985) 454-456. <https://hdl.handle.net/10278/8149>
- [31] L.Hakanson, An ecological risk index for aquatic pollution control, a sedimentological approach, *Water Research*, 14 (8) (1980) 975-1001. [https://doi.org/10.1016/0043-1354\(80\)90143-8](https://doi.org/10.1016/0043-1354(80)90143-8)
- [32] G.Young, Y.Chen, M.Yang, Concentrations, distribution, and risk assessment of heavy metals in the iron tailings of yeshan national mine park in nanjing, china, *Chemosphere*, 271 (2021) 129546. <https://doi.org/10.1016/J.chemosphere.2021.129546>
- [33] Z.Huang, S.Zheng, Y.Liu, X.Zhao, X.Qiao, C.Liu, D.Yin, Distribution, toxicity load, and risk assessment of dissolved metal in surface and overlying water at the Xiangjiang River in southern China, *Scientific reports*, 11 (1) (2021) 1-12. <https://doi.org/10.1038/S41598-020-80403-0>



- [34] L.Y.Chai, J.X.Wu, Y.J.Wu, C.B.Tang, W.C.Yang, Environmental risk assessment on slag and iron-rich matte produced from reducing-matting smelting of lead-bearing wastes and iron-rich wastes, Transactions of Nonferrous Metals Society of China, 25 (10) (2015) 3429-3435. [https://doi.org/10.1016/S1003-6326\(15\)63978-4](https://doi.org/10.1016/S1003-6326(15)63978-4)
- [35] W.K.W.Lee, J.S.J.Van.Deventer, The effects of inorganic salt contamination on the strength and durability of geopolymers, Colloids and Surfaces A: Physicochemical and Engineering Aspects, 211 (2-3) (2002) 115-126. [https://doi.org/10.1016/S0927-7757\(02\)00239-X](https://doi.org/10.1016/S0927-7757(02)00239-X)
- [36] R.K.Liew, W.L.Nam, M.Y.Chong, X.Y.Phang, M.H.Su, P.N.Y.Yek, S.S.Lam, Oil palm waste: An abundant and promising feedstock for microwave pyrolysis conversion into good quality biochar with potential multi-applications, Process Safety and Environmental Protection, 115 (2018) 57-69. <https://doi.org/10.1016/j.psep.2017.10.005>
- [37] C.Y.Heah, H.Kamarudin, A.M.Al.Bakri, M.Buhussain, M.Luqman, I.K.Nizar, Y.M.Liew, Study on solids-to-liquid and alkaline activator ratios on kaolin-based geopolymers, Construction and Building Materials, 35 (2012) 912-922. <https://doi.org/10.1016/j.conbuildmat.2012.04.102>
- [38] G.Wang, X.A.Ning, X.Lu, X.Lai, H.Cai, Y.Liu, T.Zhang, Effect of sintering temperature on mineral composition and heavy metals mobility in tailings bricks, Waste Management, 93 (2019) 112-121. <https://doi.org/10.1016/j.wasman.2019.04.001>
- [39] M.Xia, F.Muhammad, L.Zeng, S.Li, X.Huang, B.Jiao, D.Li, Solidification/stabilization of lead-zinc smelting slag in composite based geopolymer, Journal of Cleaner Production, 209 (2019) 1206-1215. <https://doi.org/10.1016/j.jclepro.2018.10.265>
- [40] Y.Sun, S.Hu, P.Zhang, K.Elmaadawy, H.Hou, Microwave enhanced solidification/stabilization of lead slag with fly ash based geopolymer, Journal of Cleaner Production, 272 (2020) 122957. <https://doi.org/10.1016/j.jclepro.2020.122957>
- [41] J.Luo, Y.Zhou, S.T.Milner, C.G.Pantano, S.H.Kim, Molecular dynamics study of correlations between IR peak position and bond parameters of silica and silicate glasses: Effects of temperature and stress, Journal of the American Ceramic Society, 101 (1) (2018) 178-188. <https://doi.org/10.1111/jace.15187>
- [42] A.Mladenovič, B.Mirtič, A.Meden, V.Z.Serjun, Calcium aluminate rich secondary stainless steel slag as a supplementary cementitious material, Construction and Building Materials, 116 (2016) 216-225. <https://doi.org/10.1016/j.conbuildmat.2016.04.141>
- [43] Y.Luo, S.Zheng, S.Ma, C.Liu, X.Wang, Preparation of sintered foamed ceramics derived entirely from coal fly ash – sciencedirect, Construction and Building Materials, 163 (2018) 529-538. <https://doi.org/10.1016/j.conbuildmat.2017.12.102>
- [44] M.Erdem, A.Özverdi, Environmental risk assessment and stabilization/solidification of zinc extraction residue: II. Stabilization/solidification, Hydrometallurgy, 105(3-4) (2011) 270-276. <https://doi.org/10.1016/j.hydromet.2010.10.014>

## PONAŠANJE PRI OČVRŠĆAVANJU I PROCENA RIZIKA PO ŽIVOTNU SREDINU TOKSIČNIH ELEMENATA JALOVINE DOBIJENIH KARBOTERMIČKOM REDUKCIJOM-MAGNETNOM SEPARACIJOM OLOVNE ŠLJAKE IZ VISOKIH PEĆI

Z.-W. Jiang <sup>a,c</sup>, M.-T. Li <sup>a,b,\*</sup>, C. Wei <sup>a,b</sup>, Y.-L. Cao <sup>a</sup>, X.-B. Li <sup>a,b</sup>, Z.-G. Deng <sup>a,b</sup>

<sup>a</sup> Fakultet za metalurško i energetska inženjerstvo, Kunming univerzitet nauke i tehnologije, Kunming, Kina

<sup>b</sup> Glavna državna laboratorija za čisto iskorišćavanje resursa kompleksnih obojenih metala, Kunming univerzitet nauke i tehnologije, Kunming, Kina

<sup>c</sup> Hunan Zhongke Electric Co.,Ltd, Juejiang, Kina

### Apstrakt

Olovna šljaka visokih peći (LBFS) nastala tokom topljenja koncentrata olova je opasan čvrsti otpad koji sadrži potencijalno toksične elemente (Pb, Zn, As i Cd) visoke pokretljivosti i rastvorljivosti. U ovoj studiji je predložen proces za iskorišćenje LBFS metodom karbotermičke redukcije-magnetne separacije. Eksperimenti toksičnosti luženja i Tessier sekvencijalne ekstrakcije sprovedeni su na LBFS i jalovini magnetne separacije (TS), a rizik po životnu sredinu je procenjen korišćenjem indeksa kodiranja procene rizika i indeksa potencijalnog ekološkog rizika. Dobijeni rezultati su pokazali da su potencijalno toksični elementi u TS očvrstnuli u spinelnoj ili silikatnoj fazi. Pored toga, XRD, SEM-EDS i FTIR rezultati su pokazali formiranje faza  $PbCa_2Si_3O_9$ ,  $ZnAl_2O_4$  i  $Ca_3(AsO_4)_2$ . Koncentracije luženja Pb, Zn, As i Cd u TS bile su mnogo niže od granica toksičnosti karakterističnog postupka luženja (TCLP) i standardnog kineskog testa luženja (CSLT). Rezultati Tesijeove sekvencijalne ekstrakcije su potvrdili da su proporcije stabilnog rezidualnog stanja potencijalno toksičnih elemenata u TS značajno veće nego u LBFS. Štaviše, nivo ekološkog rizika za životnu sredinu za TS se značajno smanjio u poređenju sa LBFS.

**Ključne reči:** Olovna šljaka iz visokih peći; Rizik po životnu sredinu; Potencijalno toksični elementi; Karbotermička redukcija; Magnetna separacija; Toksičnost luženja

